Available online at www.sciencedirect.com
SCIENCE DIRECT®
Journal of Nuclear Materials 329–333 (2004) 840–844
journal of nuclear materials
www.elsevier.com/locate/jnucmat

Transmission electron microscopy of redeposition layers on graphite tiles used for open divertor armor of JT-60

Yoshitaka Gotoh *, Takashi Arai, Junichi Yagyu, Kei Masaki, Kozo Kodama, Naoyuki Miya

JT-60 Facilities Division II, Department of Fusion Facilities, Japan Atomic Research Institute, Naka Fusion Research Establishment, 801-1 Mukouyama, Naka-machi, Naka-gun, Ibaraki-ken 311-0193, Japan

Abstract

Transmission electron microscopy, selected area electron diffraction and SEM studies were made on redeposition layers on graphite tiles removed from the lower-X-point divertor of JT-60. The observations were made, at poloidal and/or toroidal sections, in the inboard side zone of the inner-separatrix strike point. Top-surface layers of 0–6 μm-depth were correlated to the last 30-shots of the 2000-shots in the 1988 experimental campaign. In those shots, both limiter- and divertor-discharges were made with I_p below 2 MA and with neutral-beam-injection power below 25 MW. Graphene-Mo/Ti, or -Ni/Fe/Cr/Ti particulates co-deposition layers were attributed to disruptions. Columnar structures found at 20–30 mm from the strike point corresponded to divertor-discharges below 11 MW, while lamellar structures were attributed to the higher power divertor-discharges or to limiter-discharges. Columnar structures were ascribed to both low adatom-migration due to the lower redeposition temperature and the inclined incidence of carbon impurities.

1. Introduction

Erosion and redeposition in magnetic confinement nuclear-fusion experimental facilities are currently of primary importance in plasma–material interaction studies. Co-deposition of tritium with carbon impurities from wall surfaces may cause substantial increase in the in-vessel tritium inventory in fusion reactors [1]. On the other hand, since local redeposition of carbon atoms can mitigate erosion rates of divertor plates, studies on erosion/redeposition in large tokamaks are indispensable for lifetime evaluation of divertor plates in designing experimental fusion reactors. Furthermore, redeposition on plasma-facing materials may largely affect thermal response [2], as well as hydrogen trapping [3] and diffusion [4] properties. In the last decade, intensive morphological studies on redeposition layers were conducted using scanning electron microscopy (SEM) [5–7]. Meanwhile, few structural analyses were conducted by using transmission electron microscopy (TEM) [8]. Recently, morphological SEM studies on redeposition layers in the W-shaped divertor region of JAERI-Tokamak-60 Upgraded (JT-60U) after deuterium-discharge experimental phases showed multi-layers composed of 'columnar' and lamellar structures [7]. However, the sub-micrometer scale structure of the redeposition layers has not been investigated.

In the present study, nm-structure observations are made on redeposition layers formed in the lower-X-point-divertor region of JT-60 in a hydrogen discharge experimental phase in 1988. Graphite tiles operated in JT-60 in hydrogen discharge experimental campaigns, therefore without tritium contamination, were feasible for study using both TEM and a micro-sampling apparatus like the focused ion beam (FIB) facility.

* Corresponding author. Tel.: +81-29 270 7434; fax: +81-29 270 7449.
E-mail address: gotohy@dai2mc.naka.jaeri.go.jp (Y. Gotoh).

0022-3115/$ - see front matter © 2004 Elsevier B.V. All rights reserved.
doi:10.1016/j.jnucmat.2004.04.314

2. Experimental methods

2.1. Specimens

Fig. 1 shows schematically a vertical cross-sectional view of the vacuum vessel (VV) of JT-60 in June 1988–October 1988 experimental campaign. Almost 80% of the inner surface of the VV was covered with isotropic graphite tiles, with the rest, 20%, armored mostly with TiC-coated Inconel liners. Also, divertor-coil cases in the outer-divertor region on the equatorial plane were armored with TiC-coated Mo (TiC/Mo) liners. In the experimental period, nominally 1987 hydrogen discharges with both carbon-limiter and lower-X-point divertor-discharges were made, 27% of which ended in disruptions. The maximum value for the plasma current was 3.2 MA, absorbed heating power, 25.9 MW and duration time 4 s. The maximum heat flux at the divertor armor was estimated to be 5 MW/m^2. Operational temperature for the VV was typically 573 K. For the lower-X-point divertor experiments, isotropic graphite tiles (Ibiden, ETP-10) were used in divertor armor region (Fig. 1). An inset in Fig. 1 shows SEM analysis results giving redeposition-layer-thickness distribution on the lower-X-point divertor tiles as a function of poloidal distance along the tile faces. A major peak of 70 μm-thickness and a subpeak of 50 μm-thickness were found at poloidal positions of 85 and 150 mm, respectively, which corresponded to those nearly 65 mm from, and near the most frequent inner-separatrix strike-point (ISSP) zone, respectively. Specimens for TEM/SAD analyses were selected from the top-surface layers within the redeposition zones at points A and B indicated with arrows in Fig. 1. Those specimens (8 μm^W × 7 μm^L × 100 nm^T) were fabricated using a focused ion beam (FIB) apparatus (Hitachi, FB-2000) with 30 kV Ga^+-beam with the beam axis aligned normal to the tile-front face. At point A, a specimen was sectioned in the poloidal plane parallel to the minor cross-section of the torus, while, at point B, specimens were sectioned in both poloidal and toroidal planes normal to the tile-front face.

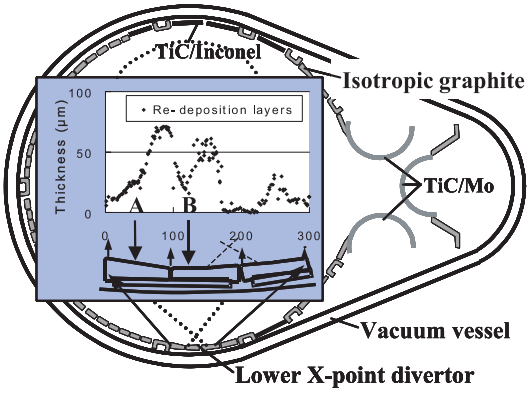

Fig. 1. A schematic view of a poloidal-section of the JT-60 vacuum vessel, showing first-wall tile installation for the June–October 1988 experimental campaign. Inset shows SEM results of redeposition thickness profile on the lower-X-point divertor tiles. Point A and B indicate poloidal positions chosen for TEM/SAD analyses.

2.2. Analysis methods

Structural and elemental analyses were conducted using a TEM (Hitachi, HF-2000) equipped with a field-emission (FE) electron source and energy-dispersive X-ray spectroscopy (EDX). The FE gun was operated at an acceleration voltage of 200 kV. Bright field images were taken by encompassing both transmitted beam and (002) reflected beam from graphite lattices. The use of FE-electron gun enabled us to obtain selected area electron diffraction (SAD) patterns from approximately 30 nm-diameter areas. SAD patterns were recorded with a camera length of 800 mm calibrated with a (110) silicon single crystal standard sample. SEM observations were made on fractured faces of redeposition layers at a rather low acceleration voltage of 4.91 V.

Each redeposition layer in a TEM image observed in a toroidal section at point B was assigned to individual shot. Thirty layers from the top surface were correlated to the last 30-shots, with the metal-codeposition layers being correlated to major and minor disruptions referring to the shot records.

3. Results and discussion

Figs. 2(a) and (b) show SEM images of poloidal fracture faces of redeposition layers on the tile at point

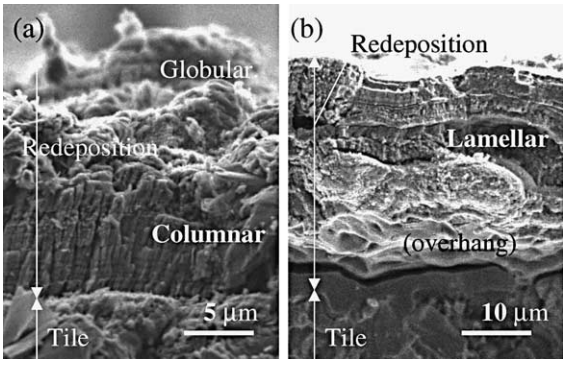

Fig. 2. SEM images of redeposition layers fractured at poloidal sections at point A (a), and B (b), in the lower-X-point divertor region of JT-60 Globular and 'columnar' textures, while lamellar structures are dominantly observed in the redeposition layers at point A, and B, respectively.

A and B (Fig. 1), respectively. Globular structure over-layers on the 'columnar' structure under-layers were observed at point A at 65 mm, on the inboard side, away from the most frequent ISSP zone. On the other hand (as shown in Fig. 2(b)), lamellar structure over-layers were found at point B, at 20–30 mm away from the most frequent ISSP zone.

Fig. 3 shows a TEM micrograph showing 0–6 μm depths layer of the redeposition layer at a poloidal section from point A. SAD patterns in 30 nm-diameter areas (indicated with arrows) are also shown. The top layers are composed of globules of around 1 μm in diameter, on the top of which thin columnar over-layers were observed. Those layers were attributed to the last 30-shots (nominal) including two divertor-discharge phases and two limiter-discharge phases. Those layers are very likely to have been modified in ordering due to disruptions. SAD patterns from the globules showed halo patterns indicating carbonaceous material of highly disordered lattice structures, probably due to the lower deposition temperatures. In the TEM images, co-deposited layers of Ni–Fe–C–Ti, or Mo–Ti particulates with graphenes were found, which were attributed to disruptions. SAD patterns from those co-deposition layers showed rather sharp (002) diffraction spots from graphite layer structure, indicating precipitation of graphenes around coagulated nm-metal particulates. Within a 5–8 μm deep layer, assigned to the third-last divertor-discharge experimental phase, layers composed of uni-directionally aligned columns with open boundaries were observed. The column axes projected on the poloidal plane were found inclined towards the outboard direction by about 20° from the tile-surface normal. The SAD patterns from the columnar layers showed (002) reflection arcs centered at 105° and 285° from the vertical direction corresponding to the tile-surface normal, indicating preferred orientation of graphene layers in the columns, around 15° to the tile-surface normal in the poloidal plane. The angle, 15°, nearly coincides with the poloidal projection angle, 20°, of the magnetic filed line in the most-inboard-side zone on the divertor-tile-surface.

Fig. 4 shows a TEM micrograph taken at a poloidal section of the redeposition layers from point B at 20–30 mm, to the inboard side, from the most frequent ISSP zone. The topmost layers in the micrograph were assigned to alternate divertor- and limiter-discharge experimental phases. Typical SAD patterns from each of those layers are also shown. Columnar structures were most obviously found in layers corresponding to the second last divertor-discharge phase, otherwise lamellar structures dominated. In the divertor-discharge layers, (002) reflection arcs is found centered at 110° and 290° in the reciprocal space, whereas those from limiter-discharge layers centered at 20° and at 200° with respect to the vertical direction in the reciprocal space that correspond to the tile-surface normal. Thus in the poloidal section of the divertor-discharge layers, graphene sheets in the columns showed preferred orientation of nearly

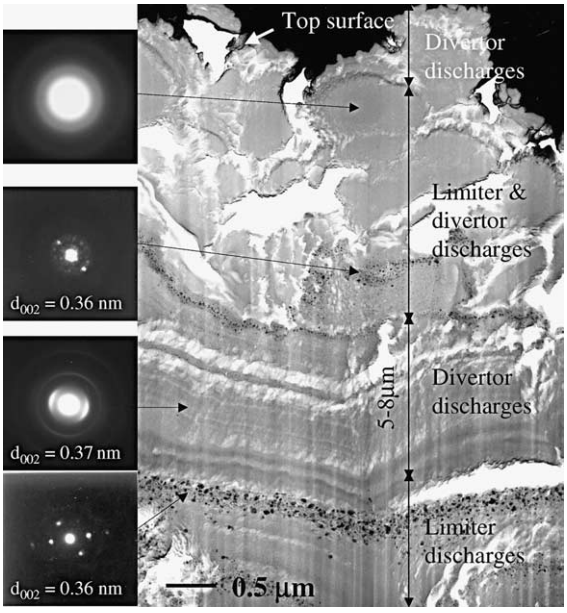

Fig. 3. TEM micrograph at a poloidal section and SAD patterns from 0 to 6 μm depth in the redeposition layers sampled from point A (Fig. 1) in the lower-X-point divertor region of JT-60.

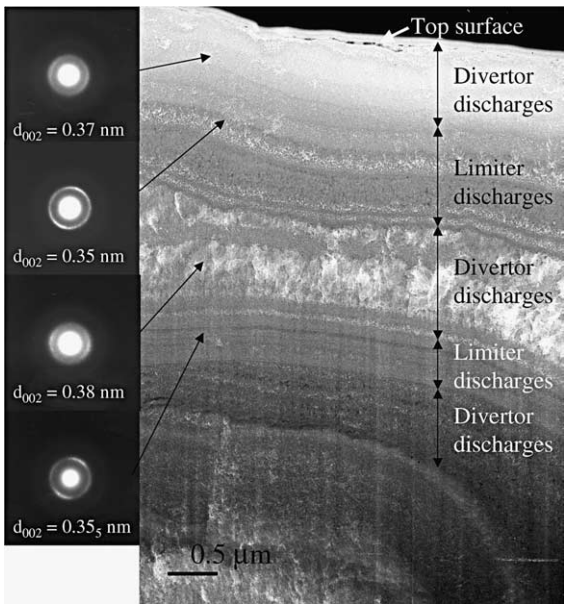

Fig. 4. TEM micrograph at a poloidal section and SAD patterns from 0 to 6 μm depth in the redeposition layers from point B (Fig. 1) in the lower-X-point divertor region of JT-60.

110° or 290° to the tile-face normal, whereas in the limiter-discharge layers, their orientations are quite opposite, rather parallel to the surface.

Fig. 5 is a high magnification TEM micrograph showing columnar layers in the redeposition layer at point B taken at a toroidal section normal to the tile-front face. A metal co-deposition over-layer and two successive columnar-structured under-layers were assigned to two successive divertor-discharges, the latter of which terminated in a disruption. Based on EDX analysis results for the metal precipitates, giving compositions as 95%Mo–3%Ti–2%Ni/Fe/Cr, those metals originated from TiC/Mo liners. In the micrograph, orientations of the column-axes were found to be inclined to the up-stream direction of the plasma current, centered at 32° with respect to the tile-face normal. From the distribution of the (002) reflection arcs in the SAD pattern in Fig. 5, the preferred orientation of graphene sheets forming the columns was estimated to be around 50° to the tile-face normal.

It is widely known that columnar-growth structure defined by columns with open-void boundaries is formed at relatively lower deposition temperatures due to low adatom mobility [9]. It was explained through ballistic aggregates, i.e. particles moving in straight lines are added to a structure whenever they touch a previously added particle [10]. In the present case, the columnar layers were found corresponding to the divertor-discharges of relatively low NBI-heating power at 6, 9, and 11 MW which very probably led surface temperature to, at most, 700 K, referring to the surface temperature data [11]. Furthermore, in the case of the ballistic aggregation on an inclined planar substrate, the upstream columns inhibit growth of the smaller columns in the shadows (self-shadowing effects), or bend their growth directions upward, off the normal direction. Those growth-inhibitions lead to formation of both open-void boundaries in-between columns and bending of some columns. Those structures can be found in the micrograph in Fig. 5.

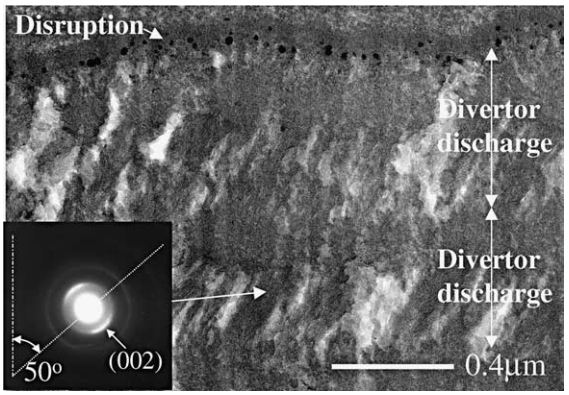

Fig. 5. TEM micrograph at the toroidal section and a SAD pattern observed for the redeposition layer at point B (Fig. 2) on the lower-X-point divertor tile of JT-60. Columnar structure layers correspond to a series of lower-X-point divertor-discharges, one shot of which ended in a disruption. Inset SAD pattern from columnar structures shows elongated diffraction spots of (002) indices of graphite, indicating that the orientation of graphite basal planes in the columns are, on average, around 50° to the tile-surface normal.

An empirical relation is known between the beam incident angle, α, with respect to the surface normal and the column-axis angle, β,

$$\tan\beta = (1/2)\tan\alpha.$$

The relation is called 'tangent rule' [10,12]. In the present case, column-axis angle β was measured to be around 32°. Assuming that graphene sheet orientations agree with beam incident angle due to possible effect of forward scattering of target carbon atoms by energetic incident impurity ions [12], beam incident angle for the carbon impurity ions, α_i, can be assumed to be 50°. It is noteworthy to point out that those α_i and β almost follows the tangent rule. All those present results are strong indications for the growth mechanisms of the observed columns: i.e. through low migration of adsorbed carbon species due to relatively lower redeposition temperatures, and through self-shadowing effects due to low angle incidence of those impurity carbon species. The preferred orientation of graphene sheets in the columns at 50° are speculated to be due to forward sputtering effects [12] of the incoming energetic ions accelerated in front of the divertor plate.

It is obvious from the TEM images of the columns with open-void boundaries that volumetric density of the columnar structure layer is considerably lower than that in the lamellar structure. The oriented graphene together with the open-void boundaries between the columns may lead to considerably higher hydrogen diffusivity through the columnar structure layers [4].

Interlayer spacing of graphitic structures in the redeposition layers can be estimated from SAD patterns in Figs. 3 and 4. Estimated average interlayer spacing, d_{002}, ranged from 0.35 to 0.38 nm. A tendency was found that d_{002} in the lamellar structures was somewhat smaller, around 0.35 nm, than those observed for the columnar structures which ranged from 0.37 to 0.38 nm. It has been shown in laboratory experiments, i.e. hydrogen-ion bombardment to saturation to graphite basal face at elevated temperatures, that d_{002} spacing in the hydrogen implantation layers decreased with increasing the irradiation temperature [13]. The observed decrease was ascribed to the decrease in densities of hydrogen atoms and hydrocarbon groups trapped within crystallites or at the boundaries. In the divertor region, divertor plate surfaces, having been exposed to high-flux hydrogen particles are to be saturated with hydrogen isotope particles at operation temperatures.

Trapped hydrogen density in the top-surface layers is considered mainly determined by surface temperature during discharges. Taking those into account, the larger interlayer spacing, d_{002} of 0.37–0.38 nm observed for the columnar layers can be assumed to be an indication for the lower redeposition temperatures for the columnar layers compared to those for the lamellar layers.

4. Conclusion

Transmission electron microscopy (TEM), selected area electron diffraction (SAD) and SEM studies were conducted on redeposition layers on graphite tiles used in the lower-X-point divertor of JT-60. The TEM observations were made, at poloidal and/or toroidal sections, in the inboard-side zone of the inner-separatrix strike point. Top-surface layers of 0–6 μm depths were analyzed correlated to the last 30-shots in the year 1988 experimental campaign. Co-deposition layers of graphene and Mo/Ti, or Ni/Fe/Cr/Ti particulates were attributed to disruptions. Columnar structures found at 20–30 mm from the strike point corresponded to the lower power divertor-discharges below 11 MW, while lamellar structures were attributed to the higher power divertor-discharges or to limiter-discharges. Columnar structures were ascribed to both low adatom-migration due to the lower redeposition temperature and the inclined incidence of the carbon impurities. Probable relations between column-axis direction and impurity-ion incidence direction were discussed. Analysis of column-axis orientation in the redeposition layers may provide us valuable information on incidence angles of incoming impurity ion species at the divertor-plate front faces.

References

[1] G. Federici et al., Nucl. Fus. 41 (2001) 1967.
[2] E. Delchambre et al. in: Proceedings of the 30th EPS Conference on Controlled Fusion and Plasma Physics, St. Petersburg, 2003, P-3.169.
[3] Y. Hirohata et al., Phys. Scr. T 103 (2003) 15.
[4] C. Martin, et al., Proc. of the 30th EPS, St. Petersburg, 2003 P-1.158.
[5] T. Ando et al., J. Nucl. Mater. 179–181 (1991) 339.
[6] J. Seggern et al., Phys. Scr. T 81 (1999) 31.
[7] Y. Gotoh et al., J. Nucl. Mater. 313–316 (1992) 637.
[8] S. Muto et al., J. Nucl. Mater. 307–311 (2002) 1289.
[9] J.A. Thornton, J. Vac. Sci. Technol. A 4 (1986) 3059.
[10] P. Ramanlal, L. Sander, Phys. Rev. Lett. 54 (1985) 1828.
[11] T. Ando et al., J. Fus. Eng. Des. 15 (1991) 39.
[12] R. Messier, J. Vac. Sci. Technol. A 18 (2000) 1538.
[13] Y. Gotoh et al., in: Proceedings of International Symposium on Carbon, Vol. II, 4–6 November 1990, Tsukuba, p. 866;
Y. Gotoh, J. Nucl. Mater. 248 (1997) 46.